

## Disease state prediction from resting state functional connectivity

R. Craddock<sup>1,2</sup>, P. Holtzheimer<sup>2</sup>, X. P. Hu<sup>3</sup>, and H. S. Mayberg<sup>2</sup>

<sup>1</sup>School of Electrical and Computer Engineering, Georgia Institute of Technology, Atlanta, Georgia, United States, <sup>2</sup>Dept. of Psychiatry and Behavioral Sciences, Emory University, Atlanta, Georgia, United States, <sup>3</sup>Dept. of Biomedical Engineering, Georgia Institute of Technology and Emory University, Atlanta, Georgia, United States

**Introduction** SVC has been applied to disease state prediction in a few cases including predicting MDD (1) and drug addiction (2) from task based fMRI measures, predicting ADHD from regional homogeneity (ReHo) measures derived from resting state BOLD (3), and predicting prenatal cocaine exposure using resting state cerebral blood flow (4). One class SVC has been applied in a density estimation setting to determine task based functional connectivity patterns that are common across a group of subjects (5). We extend this work by using SVC to predict disease state (major depression) from resting state functional connectivity patterns. Also, in an attempt to optimize the interpretation of results derived from SVC, we introduce two alternative approaches to feature selection (one filter and one wrapper approach) and compare their performance to t-test filter and recursive feature elimination.

**Methods** 40 subjects (20 depressed: MDD and 20 healthy controls: HC) participated in accordance with Institutional Review Board policy. Imaging was performed on a 3T Siemens TIM Trio scanner using a 12 channel head matrix. T1 structural images were acquired in addition to a 7 minute resting state BOLD scan. BOLD data were acquired using a ZSAGA sequence (matrix=64x64, TR=2s, TE=30ms, FA=90°, FOV=220mm, 20 axial slices, voxel resolution 3.4x3.4x4mm<sup>3</sup>, 210 measurements) to minimize susceptibility artifacts (6). During resting state subjects were asked to keep their eyes open, fixate on a point, with no other cognitive instructions (resting awake).

All preprocessing of MRI data was performed using SPM5 running in MATLAB 2008a (The Mathworks; Natick MA, USA). Anatomic scans were simultaneously segmented into white matter (WM), gray matter (GM), and cerebral-spinal fluid (CSF) and normalized to the ICBM462 normalized brain atlas. fMRI volumes were slice timing corrected, motion corrected, written into ICBM462 space using the transformation calculated on the corresponding anatomic images at 4x4x4 mm<sup>3</sup> resolution and spatially smoothed using a 6-mm FWHM Gaussian kernel. Denoising of fMRI time-courses was accomplished by regressing out motion parameters, global mean time-course, WM time-course, as well as CSF time-course. Each voxel time-course was bandpass filtered (0.009 Hz < f < 0.08 Hz) to remove frequencies not implicated in resting state functional connectivity. ROI definition and extraction was performed in AFNI (7). Fifteen ROIs were selected based on their relevance to MDD. ROIs were constructed by a clinically trained neuroanatomist (HSM) as 6-mm radius spheres using the anatomy of the ICBM462 brain anatomic template. Lateralized ROIs were chosen in the right hemisphere. For each subject ROIs were restricted to gray matter and then time-courses were extracted from every voxel in an ROI and reduced to the first eigenvariate from a singular value decomposition. This procedure was performed for every region in the ROI mask, resulting in fifteen time-courses per subject.

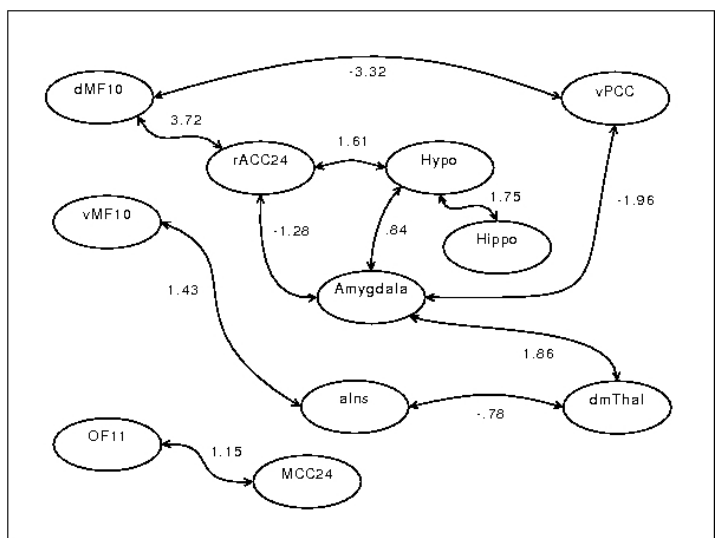
SVC of functional connectivity was performed in MATLAB using the SVM functions from the Bioinformatics Toolbox. All unique pairwise correlations of ROIs were calculated for each subject resulting in 105 correlation coefficients per subject. These data were entered into a support vector classification (SVC) analysis to discriminate MDD from HC. The linear kernel was chosen and the box constant was set to 1000 (C=1000). Results were validated using 10-fold cross validation. This procedure was repeated performed four times – one each using TF, RF, RFE and RRFE feature selection strategies. TF is performed by first calculating feature-wise t-tests to determine features that have different group means, features passing a liberal statistical threshold (p<0.05, uncorrected) are retained. RF is a multivariate approach that retains features most reliably implicated in the discriminating hyperplane calculated as determined by bootstrap confidence intervals. RFE and RRFE are wrapper feature selection procedures in which the feature set is optimized by minimizing prediction error. In each RRFE iteration, prediction error is estimated for the current feature set along with confidence intervals and score for each feature. Feature confidence intervals are used to eliminate unreliable features; if all of the features are considered reliable then RRFE defaults back to the standard RFE which removes features using the feature scores. This procedure is iterated until all features have been excluded, at which point features are chosen to minimize prediction error.

**Results** The results of SVC are shown in table 1. SVC without feature selection performed the worst and RF performed the best. TF performs better than RFE contrary to previous reports (8). The best performing implementation was able to correctly distinguish MDD from HC 100% of the time. The functional connectivity pattern that achieves this performance is illustrated in figure 1. Future work will validate these results, as well as apply SVC to predicting treatment response.

**Table 1 Results of SVC analyses**

Method	CV Prediction Error	Fleiss' Kappa	Iterations
RF	0%	-	-
RRFE	7.5%	0.69	9.5
TF	10%	-	-
RFE	22.5%	0.43	20
None	27.5%	-	-

**Figure 1. Connectivity pattern that discriminates HC from MDD**



### References:

1. Fu CHY, et al. Biol Psychiatry 2008;63(7):656-662.
2. Zhang L, et al. Proc IEEE Computer Society Conference on Computer Vision and Pattern Recognition CVPR 2005 2005;1:1211-1217.
3. Zhu CZ, et al. Med Image Comput Comput Assist Interv Int Conf Med Image Comput Assist Interv 2005;8(Pt 2):468-475.
4. Fan Y, et al. NeuroImage 2007;36(4):1189-1199.
5. Sato JR, et al. Hum Brain Mapp 2008, in press.
6. Heberlein KA, et al. Magn Reson Med 2004;51(1):212-216.
7. Cox RW. Comput Biomed Res 1996; 29:162.
8. De Martino et al. NeuroImage 2008, in press.

**Acknowledgements:** Funding and salary support from 1R01MH073719, P50MH077083, Emory URC2004113.